Cellular and Molecular Biology
E-ISSN : 1165-158X / P-ISSN : 0145-5680
www.cellmolbiol.org

Influences of microRNA-451 on the expression of HMGB1 in myocardial cells and its mechanism in ischemia-reperfusion injury

Ruiye Qiu[1*], Yajuan Zhang[2], Jun Li[1], Jun Wu[1], Ruifeng He[1]

[1] Department of Emergency, Zhuhai Integrated Traditional Chinese and Western Medicine Hospital, Zhuhai, 519020, Guangdong Province, China

[2] Department of Intensive Care Unit, Zhuhai Integrated Traditional Chinese and Western Medicine Hospital, Zhuhai, 519020, Guangdong Province, China

ARTICLE INFO

Original paper

Article history:
Received: July 13, 2023
Accepted: November 12, 2023
Published: December 31, 2023

Keywords:

High mobility group box 1 protein, immunity, ischemia-reperfusion injury, micro-ribonucleic acid, inflammatory reaction

ABSTRACT

This work aimed to understand the underlying mechanism of micro-ribonucleic acid (MicroRNA) (miR)-451 in ischemia-reperfusion injury (IRI) and the influences of miR-451 on high mobility group box 1 protein (HMGB1) in myocardial cells, 30 specific pathogen-free (SPF) male rats were selected and randomly rolled into 5 groups, which were a sham operation control (Control), an ischemia-reperfusion (I/R), aI/R+Ad-GFP, amiR-451 up-regulation (I/R+Ad-miR-451), and a miR-451 down-regulation groups (I/R+Ad-asmiR-451). There were 6 cases in each group. Myocardial cell apoptosis, the contents of serum lactic acid dehydrogenase (LDH), creatine kinase (CK), and malondialdehyde (MDA), the activity of superoxide dismutase (SOD), and the expressions of miR-451 and HMGB1mRNA were detected. Relative to those in I/R and I/R+Ad-GFP groups, the expressions of CD3+, CD4+, and CD4+/ CD8+ in I/R+Ad-miR-451 group reduced (P<0.05). The expressions of serum LDH and CK decreased (P<0.05). In contrast, MDA content and SOD activity enhanced (P<0.05). HMGB1 and Cleaved-caspase3 declined (P<0.05). Besides, miR-451 improved while the expression of HMGB1mRNA significantly reduced (P<0.05). miR-451 can regulate the expressions of HMGB1mRNA and its protein at the transcriptional level. miR-451 up-regulation can inhibit HMGB1 expression, relieve IRI, and protect myocardial cells, which may be achieved by improving oxidative stress injury and inhibiting cell apoptosis.

Doi: http://dx.doi.org/10.14715/cmb/2023.69.15.25

Introduction

Ischemia-reperfusion injury (IRI) refers to the progressive aggravation of original myocardial tissues caused by reperfusion after ischemia. IRI is related to the changes in molecules, cells, and tissues, such as cell apoptosis, inflammatory reaction, the activation of neutrophils, and oxidative stress (1,2). At present, the assessment and treatment of IRI is still one of the difficulties in clinical practice. Because the specific pathogenic mechanism of IRI is unclear, IRI is the hot topic of the current research into acute myocardial ischemia (3,4).

In recent years, high mobility group box 1 protein (HMGB1) plays a crucial role in the occurrence and progression of cardiovascular diseases as a new proinflammatory factor (5,6). The studies on IRI demonstrate that the expressions of proteins and messenger ribonucleic acid (mRNA) remarkably increased half an hour after myocardial cell hypoxia occurred (7,8). HMGB1 causes injuries to tissues by releasing proinflammatory factors (9,10). IRI can be obviously improved by different interventions of the activity of HMGB1 or its binding receptor (11,12). Hence, the verification of the influencing factors of HMGB1 up-regulation and the search for the key genes regulating HMGB1 expression can provide a new idea for the prevention of IRI (13).

microRNA is a small non-coding molecular RNA consisting of 18 to 25 nucleotides. It is involved in regulating gene expression and various biological processes of the body at the post-transcriptional level, such as cell differentiation, cell growth, and cell death (14,15). At present, multiple studies confirm that miRNAs get involved in the IRI process, such as miR-1, miR-29, miR-451, and miR-494. miRNA can regulate IRI by regulating different target genes (16,17). It is demonstrated that multiple may regulate HMGB1 expression. According to Fu et al. (18), miR-451 expression in the extracted myocardial tissues dramatically decreased in the rat IRI model. Therefore, HMGB1 may be the target gene of miR-451. The regulation of miR-451 can protect IRI through HMGB1.

Based on the above opinions, 30 Sprague-Dawley (SD) rats were selected for the construction of the I/R animal model. The research was aimed at investigating the regulatory mechanism of miR-451 in HMGB1 expression of I/R model rats and protection of I/R model rats by miR-451 up-regulation to provide an experimental basis for preventing and treating IRI clinically.

Materials and Methods

Experimental animal

30 selected specific pathogen-free (SPF) male rats were sourced from Hunan SJA Laboratory Animal Co., Ltd.. The weight of the selected rats ranged from 240g to 320g

* Corresponding author. Email: quanshabai43@163.com

with an average of 265.7±24.3g. They were 8 weeks old. SD rats were fed adaptively for 3 days with a free diet and drinking. The temperature and humidity of the animal room were kept at about 23°C and about 48°C, respectively. Besides, day lighting and night lighting were alternated.

Experimental grouping and processing

30 SD rats were grouped into 5 (6 in each), including asham operation control (control), an IRI(I/R), an I/R+Ad-GFP, miR-451 up-regulation (I/R+Ad-miR-451), and a miR-451 down-regulation groups (I/R+Ad-asmiR-451).

Rats in the Control group were only subjected to surgical operation without being induced with IRI.

Initially, 6 injection sites were identified on the frontal wall of the left ventricle of rats in the I/R group. Then, 150 μL phosphatic buffer solution (PBS) was injected. After 3 days, the left anterior descending branch (LAD) was ligated. After 30 minutes, reperfusion was performed for 24 hours.

Secondly, 6 injection sites were identified on the frontal wall of the left ventricle of rats in the I/R+Ad-GFP group. Then, 150 μ LAd-GFP was injected. After 3 days, LAD was ligated. After 30 minutes, reperfusion was performed for 24 hours.

Next, 6 injection sites were identified on the frontal wall of the left ventricle of rats in the I/R+Ad-miR-451 group. Then, 150 μL Ad-miR-451 was injected. After 3 days, LAD was ligated. After 30 minutes, reperfusion was performed for 24 hours.

Finally, 6 injection sites were identified on the frontal wall of the left ventricle of rats in the I/R+Ad-asmiR-451 group. Then, 150 μL Ad-asmiR-451 was injected. After 3 days, LAD was ligated. After 30 minutes, reperfusion was performed for 24 hours.

Construction of IRI model

The rats underwent abdominal cavity anesthesia with 3% pentobarbital sodium (purchased from The BSZH Scientific Inc., Beijing). After tracheal intubation, mechanical ventilation was carried out. Chests were ruptured and opened with the third rib forcep. A hemostatic forcep was used to clamp the intercostal artery to stop bleeding. Next, the pericardium was torn to expose the heart. LAD was found and a 6-0 stylolite was used to cross it with a depth of about 1.5 mm and a tip width of 2 mm. After that, a 1.5mm rubber tube was placed over the blood vessel with a knot tied on the rubber tube for fixation. LAD blood flow was then blocked and the chest was closed layer by layer. Next, the changes in the ST segment and cardiac rhythm in the ECG lead were observed. After 30 minutes, the wire knot was cut and reperfusion was carried out for 24 hours. The sign of successful coronary artery ligation was as follows. Cyanosis or paleness occurs in the ischemic area of the heart. Besides, the ST segment in ECG II, III, and AVF leads were elevated. The sign of successful reperfusion was as follows. The surface of the ischemic area of the heart gradually became ruddy. ECG showed that the previously elevated ST segments obviously moved down. 3mL venous blood was taken from rats' tails in fasting state and then centrifuged at 5,000 r/min for 15 minutes 7 days after the processing of the rats in 5 groups. After that, the NovoCyteflow cytometer (Agilent Technologies, Inc.) was used to measure the expressions of CD3+, CD4+, CD8+, and CD4+/ CD8+ in 5 groups.

Calculation of myocardial infarction area

The reperfusion was performed on rats for 24 hours. The silk suture indwelled in the myocardium was ligated in situ. Then, the external jugular vein was separated and 2 mL of 1% Evans blue dye was injected from the head side to the heart side via the jugular vein. After the staining, the heart was extracted and the cardiac atrium and right ventricle were removed. After that, the heart was cleansed with physiological saline and then frozen at -80°C for 30 minutes. The heart was taken out and the left ventricle was cut into 5 to 6 transverse sections with a thickness of 2mm along the major axis of the heart. Then, the transverse sections were put into 1% 2,3,5-triphenyltetrazolium chloride (TTC) and stored away from light at 37°C for incubation for 15 minutes. When the sections were stained red, cardiac tissues were rinsed with physiological saline and then fixed in 4% polyformaldehyde (POM) (SenBeiJia Biological Technology Co., Ltd.) overnight. Next, a computer-aided image analysis system (Image-Pro Plus3.0) was used for the measurement of the unischemic myocardial tissue area (blue area), infarction area (white area), and ischemic area (red and white area). Besides, the proportions of the areas of the infarction area and ischemic area in myocardial tissues were calculated to estimate the myocardial infarction area. Finally, hematoxylin-eosin staining (HE staining) was adopted for the morphological observation of myocardial tissues.

Assessment of myocardial cell apoptosis by TdT-mediated dUTP nick end labeling (TUNEL) staining

TUNEL cell apoptosis detection kit (purchased from Shuoheng Biotechnology Co., Ltd., Guangzhou) was used for the detection of the rupture of nucleus DNA during the early apoptosis of sectioned myocardial cells.

Myocardial sections were placed into a constant-temperature oven at 65°C and then baked for 1 hour. Next, they were successively soaked in xylene I and II for 15 minutes, respectively and 100%, 95%, 85%, and 75% ethanol for 5 minutes. Myocardial sections were rinsed with running water for 10 minutes. Sections were incubated in a protease working solution for 20 minutes. Then, they were added with 50μL TUNEL reaction mixture and incubated away from light in a biochemical incubator at 37°C for 60 minutes. Next, myocardial sections were cleansed with PBS 3 times and then added with 50 μL transformed peroxidase (POD) solution. The myocardial sections were incubated at 37°C for 30 minutes. Then, myocardial sections were cleansed with PBS 3 times and added with 50 μL 3,3 diaminobenzidine (DAB) (purchased from Suzhou Yacoo Science Co., Ltd.) substrate. Myocardial sections were stained again with hematoxylin and then dehydrated, transparentized, and sealed for observation under a light microscope. Next, the cells with positive TUNEL results and all cells in 10 fields of view were counted. Besides, the myocardial cell apoptosis index was calculated.

Measurement of the markers for myocardial tissue injury in serum (LDH and CK)

Before and after the production of all rat I/R models, 2 mL of blood was extracted from the external jugular vein before ischemia and 24 hours after reperfusion. Then, the extracted blood was placed in a coagulation tube at room

temperature for 15 minutes. After that, it was centrifuged. The upper light yellowish transparent serum was extracted and then frozen in a refrigerator at -80°C. According to serum LDH and CK detection kit (Zhejiang IKON Biotechnology Co., Ltd.) instructions, samples and reaction reagents were added. Besides, a microplate reader was utilized to measure absorbance value. The concentrations of LDH and CK samples were calculated.

Measurement of malondialdehyde (MDA) content and superoxide dismutase (SOD) activity

100 mg myocardial tissues were extracted from all groups and then added with physiological saline. Then, they were placed into a glass homogenizer and stirred into 10% myocardial tissue homogenate. Next, the myocardial tissue homogenate was centrifuged on ice at 4,000 rmp/min for 15 minutes. According to MDA and SOD kit (Nanjing Jiancheng Bioengineering Institute) instructions, xanthine oxidation and thiobarbituric acid methods were adopted to measure SOD activity and the content of MDA, which were set as the indexes for the expressions of oxygen free radical and lipid hydroperoxide in myocardial tissues (equations 1 and 2).

$$Activity\ of\ SOD\ in\ tissues(U/mg) = \left\{\begin{array}{l}\left[(Control\ tube\ absorbance)-(Measure\ tube\ absorbance)/(Control\ tube\ absorbance)\times 50\%\right]\\ \times[Total\ volume\ of\ reaction\ solution/Sample\ loading(mL)]\end{array}\right\} /Tissue\ protein\ content(mg/mL) \quad [1]$$

$$MDA\ content\ in\ tissue(nmol/mg) = \left\{\begin{array}{l}\left[(Measure\ tube\ absorbance)-(Measure\ absorbance\ of\ blank\ tube)\right]/\\ \left[(S\tan dard\ tube\ absorbance)-(Absorbance\ of\ s\tan dard\ tube)\right]\times\\ \left[S\tan dard\ concentration(10nmol/L)\right]\end{array}\right\} /Tissue\ protein\ content(mg/mL) \quad [2]$$

Detection of the expressions of miR-451 and HMGB-1mRNA using real-time polymerase chain reaction (PCR) method

After liquid nitrogen was extracted and quickly frozen, 100mg myocardial tissues in the ischemic area were frozen at -80°C in a refrigerator and then cut into pieces on ice. After that, the myocardial tissues were added with 1mL Trizol solution and homogenized with a glass homogenizer. Next, total RNA was extracted for quantification and purity identification. A complementary RNA (cRNA) chain was synthesized and the Real-time PCR method was used for the detection of the expressions of miR-451 and HMGB1mRNA in myocardial tissues. The results were expressed as $2^{-\Delta\Delta Ct}$. The quantification expression of mRNA was calculated.

Detection of the expressions of HMGB1 and Caspase-3 proteins in myocardial tissues by Western Blotting method

After liquid nitrogen was extracted and quickly frozen, 100mg myocardial tissues in the ischemic area were frozen at -80°C in a refrigerator and then cut into pieces on ice. After that, they were added with radioimmunoprecipitation assay (RIPA) cell lysis solution containing 1mL phenylmethylsulfonyl fluoride (PMSF) and homogenized on a glass grinder. Next, HMGB1 and Caspase-3 antibodies were used to detect the contents of HMGB1 and Caspase-3. Western Blotting was employed for the analysis. GAPDH expression was set as an internal standard. Besides, relative expressions of HMGB1 and Caspase-3 were calculated.

Statistical methods

Excel was used to set up a database for all research data. SPSS21.0 was employed for data analysis. Measurement data were expressed as mean±standard deviation ($\bar{x}\pm s$). Enumeration data were analyzed with χ^2 test and denoted by percentage (%). $P<0.05$ revealed that differences indicated statistical significance.

Results

Measurement of myocardial infarction area

Figure 1 compares the measurements of myocardial infarction areas in various groups. As it revealed, after 24-hour reperfusion, the myocardial infarction area induced by rat myocardial injury in the I/R +Ad-miR-451 group reduced more remarkably than that in the I/R and I/R+Ad-GFP groups ($P<0.05$). No apparent change was detected in the myocardial infarction area inI/R+Ad-asmiR-451 group ($P>0.05$).

Inflammatory infiltration of myocardial tissues

The inflammatory infiltration of sample tissues was analyzed, as demonstrated in Figure 2 below. It was demonstrated that myocardial cell staining was normal among the rats in the Control group. Besides, the cells were arranged regularly and tightly. The nucleus had clear boundaries without obvious infiltration of inflammatory cells and injured areas. In contrast, myocardial cells were disordered with

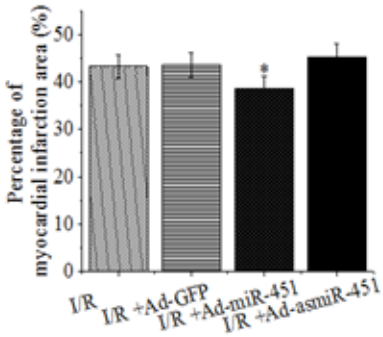

Figure 1. The proportion of myocardial infarction area after the processing of the Ad-miR-451 group. Note: The comparison with myocardial infarction area in I/R and I/R+Ad-GFP groups demonstrated *$P<0.05$.

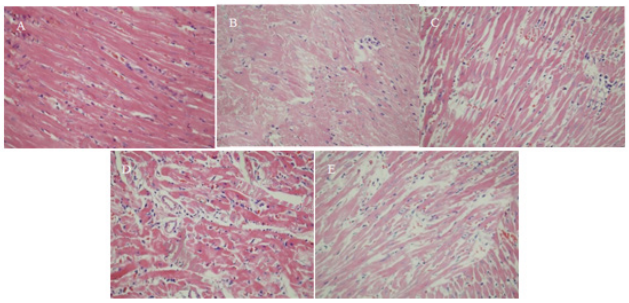

Figure 2. Morphological changes in myocardial tissues among rats in all groups (HE staining, ×200). (A) Control group. (B) I/R group. (C) I/R+Ad-GFP group. (D) I/R+Ad-miR-451 group. (E) I/R +Ad-asmiR-451 group.

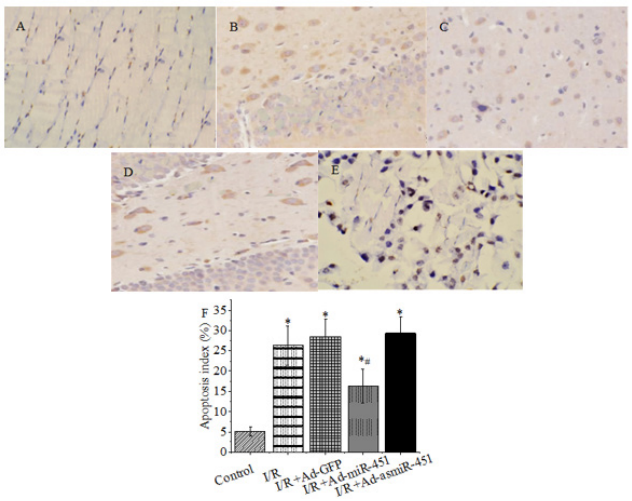

Figure 3. Myocardial cell apoptosis among rats detected by TUNEL method (×400). (A) Control group. (B) I/R group. (C) I/R+Ad-GFP group. (D) I/R+Ad-miR-451 group. (E) I/R+Ad-asmiR-451 group. (F) Myocardial cell apoptosis indexes of rats. Note: The comparison with the apoptosis index in the Control group showed *P<0.05. The comparison with myocardial cell apoptosis indexes in I/R and I/R+Ad-GFP groups demonstrated #P<0.05.

different levels of swelling and blurred boundaries of the nucleus in I/R and I/R+Ad-GFP groups. Myocardial cells showed mild swelling with the infiltration of a few neutrophils in the I/R+Ad-miR-451 group. Besides, myocardial cells were disordered and the infiltration of neutrophils increased in the I/R+Ad-asmiR-451 group.

Detection of rat myocardial cell apoptosis by TUNEL method

After 24-hour reperfusion, sporadic apoptotic cells were detected in the Control group. Apoptosis indexes in the other four groups were all superior to those in the Control group (P<0.05). Versus that in I/R and I/R+Ad-GFP groups, apoptosis indexes of myocardial cells in the I/R+Ad-miR-451 group decreased (P<0.05). Myocardial cell apoptosis indexes in the I/R+Ad-asmiR-451 group indicated no statistical significance (P>0.05). These results are displayed in Figure 3 below.

Comparison of the expressions of immune cells of rats in all groups

It was found that the Control group exhibited lower expressions of CD3+, CD4+, and CD4+/ CD8+ to other groups (P<0.05). Relative to those in I/R and I/R+Ad-GFP groups, CD3+, CD4+, and CD4+/ CD8+ in I/R+Ad-miR-451 group decreased (P<0.05). CD8+ in I/R, I/R+Ad-GFP, I/R+Ad-miR-451, and I/R+Ad-asmiR-451 groups were all inferior to that in Control group (P<0.05). Besides, CD8+ in I/R +Ad-asmiR-451 group didn't change significantly relative to that in I/R and I/R+Ad-GFP groups (P>0.05) (Figure 4).

Influences of miR-451 on the concentrations of serum LDH and CK

In this work, the impacts of miR-451 on the concentrations of serum LDH and CK were analyzed and summarized in Figure 5 below. After 24-hour reperfusion, the concentrations of LDH and CK in I/R and I/R+Ad-GFP groups enhanced based on those in the Control

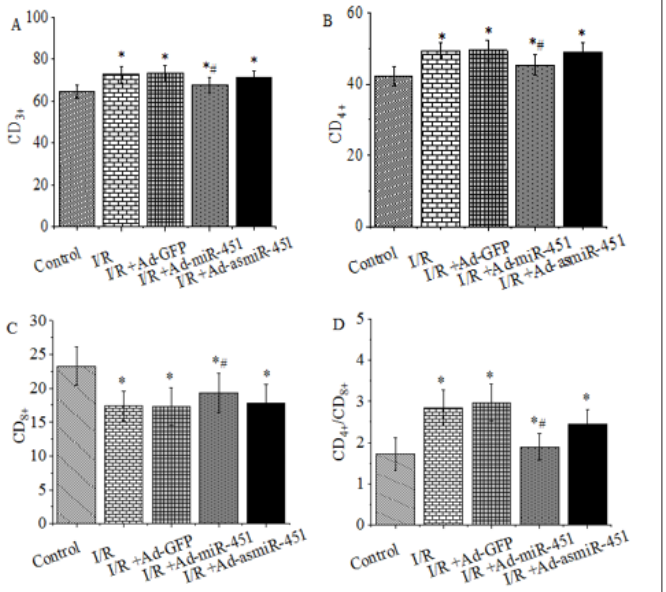

Figure 4. Comparison of immune cell expressions of rats in all groups. (A) CD3+lymphocyte. (B) CD4+lymphocyte. (C) CD8+lymphocyte. (D) The ratio of CD4+ to CD8+. Note: The comparison with the expressions of immune cells in Control group indicated *P<0.05. The comparison with immune cell expressions in I/R and I/R+Ad-GFP groups showed #P<0.05.

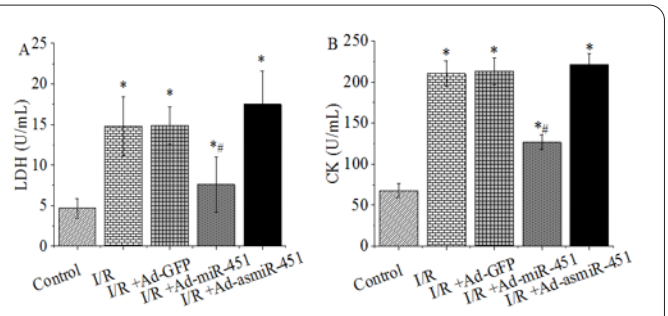

Figure 5. Changes in LDH and CK expressions among rats in all groups. (A) LDH concentration. (B) CK concentration. Note: The comparison with the concentrations of LDH and CK in Control group showed *P<0.05. The comparison with concentrations of LDH and CK in I/R and I/R+Ad-GFP groups revealed #P<0.05.

group(P<0.05). Based on those in I/R and I/R+Ad-GFP groups, LDH and CK concentrations in I/R+Ad-miR-451 group reduced (P<0.05). LDH and CK concentrations in I/R+Ad-asmiR-451 increased without statistical significance (P>0.05).

Influences of miR-451 on MDA content and SOD activity in myocardial tissues

Following a 24-hour reperfusion, MDA contents in I/R and I/R +Ad-GFP groups obviously enhanced relative to those in Control group, while SOD activity apparently decreased (P<0.05). Relative to those in I/R and I/R+Ad-GFP groups, MDA content and SOD activity improved in I/R+Ad-miR-451 group (P<0.05). MDA content enhanced while SOD activity declined in I/R +Ad-asmiR-451 group (P>0.05). The above descriptions are depicted in Figure 6.

Influences of miR-451 on the expressions of HMGB1 and Cleaved-caspase3 in myocardial tissues

After 24-hour reperfusion, the expressions of HMGB1 and Cleaved-caspase3 in I/R and I/R +Ad-GFP groups

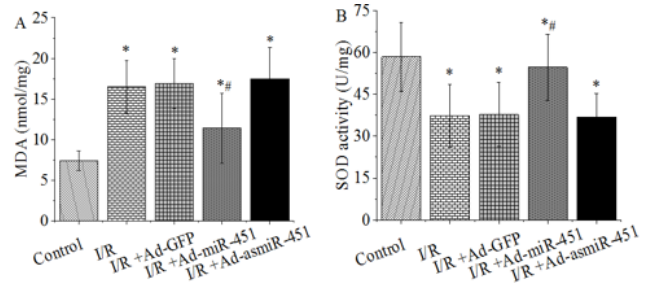

Figure 6. Influences of miR-451 on MDA content (A) and SOD activity (B). Note: The comparison in Control group revealed **P*<0.05. The comparison with those in I/R and I/R +Ad-GFP groups indicated #*P*<0.05.

obviously increased based on those in Control group (*P*<0.05). Based on those in I/R and I/R+Ad-GFP groups, HMGB1 and Cleaved-caspase3 in I/R+Ad-miR-451 group remarkably reduced (*P*<0.05). HMGB1 and Cleaved-caspase3 in I/R+Ad-asmiR-451 group enhanced (*P*>0.05). The results described herein are explained in Figure 7.

Expressions of miR-451 in myocardial tissues in all groups and influences of the expressions of miR-451 in myocardial tissues on the expression of HMGB1mRNA

Relative to that in Control group, miR-451 in I/R, I/R+Ad-GFP, I/R+Ad-miR-451, and I/R+Ad-asmiR-451 groups apparently reduced (*P*<0.05). Versus that in I/Rand I/R+Ad-GFP groups, miR-451 in I/R+Ad-miR-451 group notably enhanced (*P*<0.05). Versus that in I/R and I/R+Ad-GFP groups, miR-451 in I/R+Ad-asmiR-451 group notably reduced (*P*<0.05).

Versus that in Control group, HMGB1mRNA in other groups apparently improved (*P*<0.05). Relative to that in I/R and I/R+Ad-GFP groups, HMGB1mRNA in I/R+Ad-miR-451 group obviously decreased (*P*<0.05). Versus that in I/R and I/R +Ad-GFP groups, HMGB1mRNA in I/R+Ad-asmiR-451 group remarkably enhanced (*P*<0.05) (Figure 8).

Discussion

With the development and progress of vascular recanalization therapy, myocardial ischemia-reperfusion becomes one of the risk factors for therapeutic effect on acute myocardial ischemia (19). In the early stage of IRI, an increasing number of reactive oxygen species appear in cells. Besides, inflammatory cells are activated and cell apoptosis and necrosis occur frequently. In the late stage of IRI, compensatory hypertrophy of cells leads to myocardial hypertrophy after myocardial cell apoptosis (20-22). Hence, improving myocardial ischemia-reperfusion for patients becomes the top priority in the treatment of acute myocardial ischemia. miR-451 is abundant in myocardial cells. According to previous data, miR-451 gets involved in the oxidative stress process of myocardial ischemia-reperfusion and relieves the symptoms of myocardial ischemia-reperfusion by regulating relevant target proteins in apoptosis pathways (23). The established I/R rat models confirmed that miR-451 cold improve oxidative stress injuries and apoptosis of myocardial cells by regulating HMGB1 at the transcriptional level.

miRNA could regulate the expressions of specific target genes at the transcriptional level or epigenetic level. Mu et

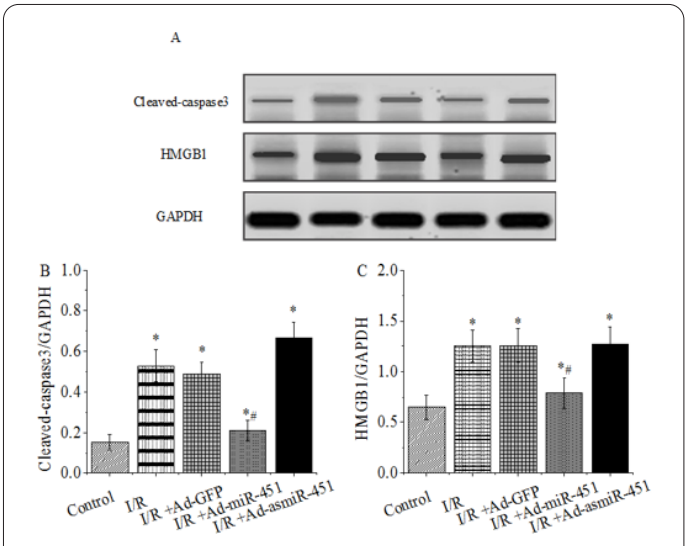

Figure 7. Expressions of HMGB1 and Cleaved-caspase3 proteins of rats in all groups. (A) Relative expressions of HMGB1 and Cleaved-caspase3 in all groups. (B) Comparison of the expressions of HMGB1 among all groups. (C) Comparison of the expressions of Cleaved-caspase3 among all groups. Note: The comparison with the expressions of HMGB1 and Cleaved-caspase3 in Control group demonstrated **P*<0.05. The comparison with HMGB1 and Cleaved-caspase3 in I/R and I/R +Ad-GFP groups indicated #*P*<0.05.

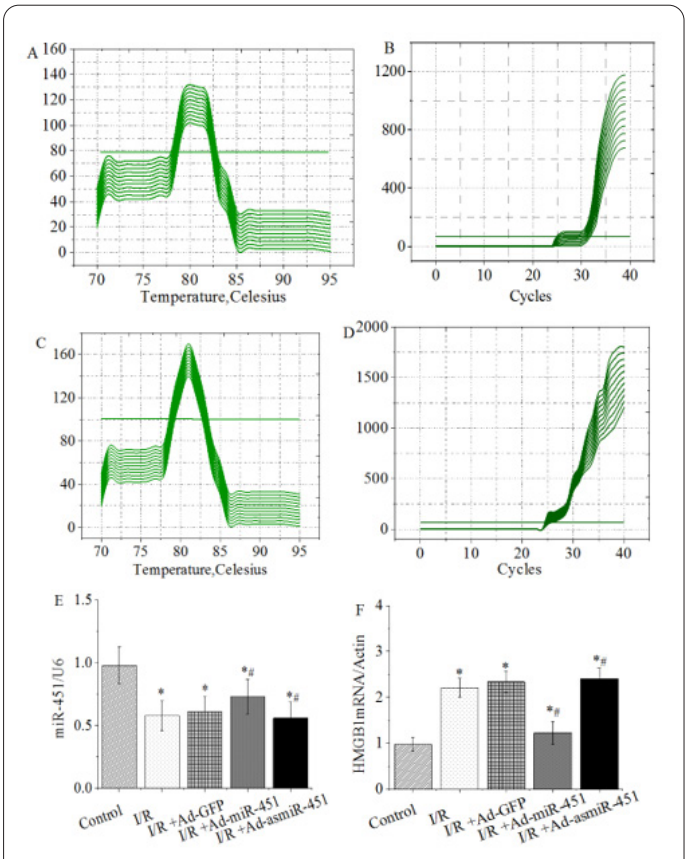

Figure 8. Expressions of miR-451 in myocardial tissues in all groups and the influences of the expressions of miR-451 in myocardial tissues on the expression of HMGB1mRNA. (A) miR-451solubility curves. (B) miR-451 amplification curves. (C) HMGB1mRNA solubility curves. (D) miR-451 amplification curves. (E) Expressions of miR-451 in myocardial tissues in all groups. (F) Influences of miR-451 expression on HMGB1mRNA expression. Note: The comparison with the expressions of miR-451 and HMGB1mRNA in Control group showed **P*<0.05. The comparison with miR-451 and HMGB-1mRNA in I/R and I/R+Ad-GFP groups revealed #*P*<0.05.

al. (24) verified that miR-451 regulated the expression of the target gene CUGBP in the form of a gene cluster in the myocardial cells of myocardial ischemia-reperfusion rat models. Consequently, the downstream anti-apoptotic gene COX was regulated and the myocardial cell apoptosis rate was reduced. In addition, pre-processing of myocardial cells with mimetic agent miR-451 could remarkably inhibit the expression of target gene Rac-1 to down-regulate the activity of oxidase NAPDH and avoid the injury of oxygen-free radicals (25-27). The research results demonstrated that the expressions of HMGB1mRNA and its proteins both decreased after the up-regulation of miR-451 in myocardial ischemia-reperfusion rat models (P<0.05). HE staining was used for the observation of infiltration of inflammatory cells in myocardial tissues among I/R model rats. Different levels of the infiltration of inflammatory cells occurred in myocardial tissues among the rats in all groups other than Control group after the successful construction of myocardial ischemia-reperfusion models. Relative to that in I/R and I/R+Ad-GFP groups, myocardial infarction area of I/R+Ad-miR-451 group reduced (P<0.05). Based on those in Control group, LDH and CK and MDA contents in other groups decreased, while SOD activity improved, which was consistent with the study outcomes obtained by Jia et al. (28). The above finding indicated that up-regulating miR-451 expression could protect myocardial cells by down-regulating HMGB1. The protection mechanism might be the alleviation of inflammatory reactions, the reduction in oxidative stress injury, or the inhibition of cell apoptosis.

Active and effective treatment methods can prevent and treat myocardial ischemia-reperfusion, improve surgical success rate, and accelerate the rehabilitation of patients. Inflammatory reaction and immunology mechanisms are the key mechanisms of IRI. Neutrophil is the main inflammatory cell in IRI. However, the latest study shows that lymphocyte plays a significant role in IRI. Hence, early effective inhibition of lymphocyte aggregation can prevent the occurrence of IRI. According to the research results, the expressions of CD3+, CD4+, and CD4+/CD8+ in I/R, I/R+Ad-GFP, I/R+Ad-miR-451, and I/R+Ad-asmiR-451 groups were all superior to those in Control group (P<0.05). Versus those in I/R and I/R+Ad-GFP groups, CD3+, CD4+, and CD4+/CD8+ in I/R+Ad-miR-451 group reduced (P<0.05). It was indicated that I/R models were successfully constructed and the accumulation of CD3+ and CD4+ were accelerated. Up-regulating miR-451 expression could inhibit the aggregation of lymphocytes CD3+ and CD4+, reduce IRI, and protect myocardial cells.

The limitation of this research lies in the markedly upshifted HMGB1 proteins in I/R+Ad-asmiR-451 group relative to that in I/R and I/R +Ad-GFP groups without statistical significance, which may be caused by the small sample size of animals included in the experiment.

The research was aimed at investigating the regulatory mechanism of miR-451 in HMGB1 among rats with IRI and the protection of I/R rat model by the up-regulation of miR-451 expression. It was verified that miR-451 could regulate HMGB1mRNA and the expressions of its proteins at the transcriptional level. The up-regulation of miR-451 could inhibit HMGB1 expression, reduce IRI, and protect myocardial cells, which might be achieved by improving oxidative stress injuries of cells and inhibiting cell apoptosis. The limitation of this research lies in the small sample size of experimental animals, which may result in the lack of statistical significance. In follow-up research, the sample size needs to be expanded for further investigation and verification of the accuracy of the conclusion.

References

1. Jiménez-Castro MB, Cornide-Petronio ME, Gracia-Sancho J, Peralta C. Inflammasome-mediated inflammation in liver ischemia-reperfusion injury. Cells 2019; 8(10): 1131. https://doi.org/10.3390/cells8101131
2. Lv S, Liu H, Wang H. The interplay between autophagy and NLRP3 inflammasome in ischemia/reperfusion injury. Int J Mol Sci 2021; 22(16): 8773. https://doi.org/10.3390/ijms22168773
3. Liang S, Wang Y, Liu Y. Dexmedetomidine alleviates lung ischemia-reperfusion injury in rats by activating PI3K/Akt pathway. Eur Rev Med Pharmacol Sci 2019; 23(1): 370-377. https://doi.org/10.26355/eurrev_201901_16785
4. Paudel YN, Angelopoulou E, C BK, Piperi C, Othman I. High mobility group box 1 (HMGB1) protein in Multiple Sclerosis (MS): mechanisms and therapeutic potential. Life Sci 2019; 238: 116924. https://doi.org/10.1016/j.lfs.2019.116924
5. Mandke P, Vasquez KM. Interactions of high mobility group box protein 1 (HMGB1) with nucleic acids: Implications in DNA repair and immune responses. DNA Repair (Amst) 2019; 83: 102701. https://doi.org/10.1016/j.dnarep.2019.102701
6. Ge Y, Huang M, Yao YM. The effect and regulatory mechanism of high mobility group Box-1 protein on immune cells in inflammatory diseases. Cells 2021; 10(5): 1044. https://doi.org/10.3390/cells10051044
7. Angelopoulou E, Paudel YN, Piperi C. Exploring the role of high-mobility group box 1 (HMGB1) protein in the pathogenesis of Huntington's disease. J Mol Med (Berl) 2020; 98(3): 325-334. https://doi.org/10.1007/s00109-020-01885-z
8. Andersson U, Yang H, Harris H. High-mobility group box 1 protein (HMGB1) operates as an alarmin outside as well as inside cells. Semin Immunol 2018; 38: 40-48. https://doi.org/10.1016/j.smim.2018.02.011
9. Wu Y, Wang HB, Yang Y, Dong QL. Effect of serum high mobility group box 1 protein on immune function and autophagy level of myocardial cells in rats with sepsis. Eur Rev Med Pharmacol Sci 2021; 25(4): 2065-2071. https://doi.org/10.26355/eurrev_202102_25111
10. Chen Z, Li R, Pei LG, Wei ZH, Xie J, Wu H, Xu B. High-mobility group box-1 promotes vascular calcification in diabetic mice via endoplasmic reticulum stress. J Cell Mol Med 2021; 25(8): 3724-3734. https://doi.org/10.1111/jcmm.16075
11. Bai H, Wu S. miR-451: a novel biomarker and potential therapeutic target for cancer. Onco Targets Ther 2019; 12: 11069-11082. https://doi.org/10.2147/OTT.S230963
12. Lv XW, He ZF, Zhu PP, Qin QY, Han YX, Xu TT. miR-451-3p alleviates myocardial ischemia/reperfusion injury by inhibiting MAP1LC3B-mediated autophagy. Inflamm Res 2021; 70(10-12): 1089-1100. https://doi.org/10.1007/s00011-021-01508-4
13. Guo R, Gu J, Zhang Z, Wang Y, Gu C. MiR-451 promotes cell proliferation and metastasis in pancreatic cancer through targeting CAB39. Biomed Res Int 2017; 2017: 2381482. https://doi.org/10.1155/2017/2381482
14. Wang L, Zhang J, Sun H, Ji X, Zhang S. Effect of miR-451 on IVF/ICSI-ET outcome in patient with endometriosis and infertility. Am J Transl Res 2021; 13(11): 13051-13058.
15. Guo Y, Gao J, Liu Y, Zhang X, An X, Zhou J, Su P. miR-451 on myocardial ischemia-reperfusion in rats by regulating AMPK

signaling pathway. Biomed Res Int 2021; 2021: 9933998. https://doi.org/10.1155/2021/9933998

16. Zhang Y, Chu X, Wei Q. MiR-451 promotes cell apoptosis and inhibits autophagy in pediatric acute myeloid leukemia by targeting HMGB1. J Environ Pathol Toxicol Oncol 2021; 40(2): 45-53. https://doi.org/10.1615/JEnvironPatholToxicolOncol.2021037139
17. Duan Y, Zhang Y, Peng W, Jiang P, Deng Z, Wu C. MiR-7-5pand miR-451 as diagnostic biomarkers for papillary thyroid carcinoma in formalin-fixed paraffin-embedded tissues. Pharmazie 2020; 75(6): 266-270. https://doi.org/10.1691/ph.2020.0335
18. Fu C, Chen S, Cai N, Liu Z, Wang P, Zhao J. Potential neuroprotective effect of miR-451 against cerebral ischemia/reperfusion injury in stroke patients and a mouse model. World Neurosurg 2019; 130: e54-e61. https://doi.org/10.1016/j.wneu.2019.05.194
19. Liu Q, Hu Y, Zhang M, Yan Y, Yu H, Ge L. microRNA-451 protects neurons against ischemia/reperfusion injury-induced cell death by targeting CELF2. Neuropsychiatr Dis Treat 2018; 14: 2773-2782. https://doi.org/10.2147/NDT.S173632
20. Kiss A, Heber S, Kramer AM, Hackl M, Skalicky S, Hallström S, Podesser BK, Santer D. MicroRNA expression profile changes after cardiopulmonary bypass and ischemia/reperfusion-injury in a porcine model of cardioplegic arrest. Diagnostics (Basel) 2020; 10(4): 240. https://doi.org/10.3390/diagnostics10040240
21. Cao J, Da Y, Li H, Peng Y, Hu X. Upregulation of microRNA-451 attenuates myocardial I/R injury by suppressing HMGB1. PLoS One 2020; 15(7): e0235614. https://doi.org/10.1371/journal.pone.0235614
22. Meng K, Jiao J, Zhu RR, Wang BY, Mao XB, Zhong YC, Zhu ZF, Yu KW, Ding Y, Xu WB, Yu J, Zeng QT, Peng YD. The long noncoding RNA hotair regulates oxidative stress and cardiac myocyte apoptosis during ischemia-reperfusion injury. Oxid Med Cell Longev 2020; 2020: 1645249. https://doi.org/10.1155/2020/1645249
23. Zhu XH, Han LX, Zhang RJ, Zhang P, Chen FG, Yu J, Luo H, Han XW. The functional activity of donor kidneys is negatively regulated by microribonucleic acid-451 in different perfusion methods to inhibit adenosine triphosphate metabolism and the proliferation of HK2 cells. Bioengineered 2022; 13(5): 12706-12717. https://doi.org/10.1080/21655979.2022.2068739
24. Mu Y, Yin TL, Zhang Y, Yang J, Wu YT. Diet-induced obesity impairs spermatogenesis: the critical role of NLRP3 in Sertoli cells. Inflamm Regen 2022; 42(1): 24. https://doi.org/10.1186/s41232-022-00203-z
25. Wan P, Su W, Zhang Y, Li Z, Deng C, Li J, Jiang N, Huang S, Long E, Zhuo Y. LncRNA H19 initiates microglial pyroptosis and neuronal death in retinal ischemia/reperfusion injury. Cell Death Differ 2023; 30(3): 859. https://doi.org/10.1038/s41418-022-01105-w
26. Song Y, Li Z, He T, Qu M, Jiang L, Li W, Shi X, Pan J, Zhang L, Wang Y, Zhang Z, Tang Y, Yang GY. M2 microglia-derived exosomes protect the mouse brain from ischemia-reperfusion injury via exosomal miR-124. Theranostics 2019; 9(10): 2910-2923. https://doi.org/10.7150/thno.30879
27. Gong C, Zhou X, Lai S, Wang L, Liu J. Long noncoding RNA/Circular RNA-miRNA-mRNA axes in ischemia-reperfusion injury. Biomed Res Int 2020; 2020: 8838524. https://doi.org/10.1155/2020/8838524
28. Jia S, He D, Liang X, Cheng P, Liu J, Chen M, Wang C, Zhang H, Meng C. Corilagin induces apoptosis and inhibits autophagy of HL-60 cells by regulating miR-451/HMGB1 axis. Mol Med Rep 2022; 25(1): 34. https://doi.org/10.3892/mmr.2021.12550